JOC Article

Self-Assembly Dynamics of Modular Homoditopic Bis-calix[5]arenes and Long-Chain α,ω-Alkanediyldiammonium Components

Giuseppe Gattuso,[†] Anna Notti,[†] Andrea Pappalardo,[†,‡] Melchiorre F. Parisi,*[,†] Ilenia Pisagatti,[†] Sebastiano Pappalardo,*[,§] Domenico Garozzo,[||] Angela Messina,[||] Yoram Cohen,*[,⊥] and Sarit Slovak[⊥]

Dipartimento di Chimica Organica e Biologica, Università di Messina, Salita Sperone 31, 98166 Messina, Italy, Dipartimento di Scienze Chimiche, Università di Catania, Viale A. Doria 6, 95125 Catania, Italy, CNR, ICTP Catania, Viale Regina Margherita 6, 95125 Catania, Italy, and School of Chemistry, The Raymond and Beverly Sackler Faculty of Exact Sciences, Tel Aviv University, Ramat Aviv 69978, Tel Aviv, Israel

mparisi@unime.it; spappalardo@dipchi.unict.it; ycohen@post.tau.ac.il

Received June 6, 2008

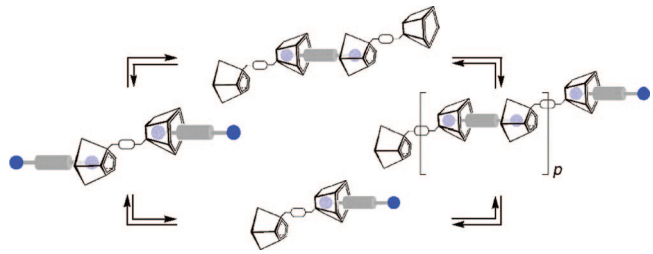

Homoditopic building blocks **1**, featuring two π-rich cone-like calix[5]arene moieties connected at their narrow rims by a rigid *o*-, *m*-, or *p*-xylyl spacer in a centrosymmetric divergent arrangement, show a remarkable tendency to spontaneously and reversibly self-assemble with the complementary homoditopic α,ω-alkanediyldiammonium dipicrate guest salts $\mathbf{C_8}-\mathbf{C_{12}}\cdot$2Pic through iterative intermolecular inclusion events, forming supramolecular assemblies whose composition and dynamics strongly depend upon the length of the connector, the geometry of the spacer, as well as the concentration and/or molar ratios between the two components. ^{1}H NMR spectroscopy and ESI-MS studies of $\mathbf{1/C}_n\cdot$2Pic modular homoditopic pairs support the formation of discrete (bis)-*endo*-cavity assemblies with the shorter $\mathbf{C_8}$ and $\mathbf{C_9}$ connectors, and/or (poly)capsular assemblies with the longer $\mathbf{C_{10}}-\mathbf{C_{12}}$ components under appropriate concentrations and molar ratios (50 mM equimolar solutions). ^{1}H NMR titration experiments and diffusion NMR studies provide clear evidence for the self-assembly dynamics of the complementary pairs here investigated.

Introduction

The reversible and thermodynamically controlled construction of supramolecular assemblies from pairs of building blocks displaying complementary molecular affinities is a current challenge in noncovalent synthesis.[1] Noncovalent forces are known to play a major role in promoting the self-organization and stabilization of biological systems. Nature constructs its most spectacular structures—enzymes, membranes, channels, etc.—by making use of the reversible assembly of self-complementary subunits, which store within their covalent structure the information needed for the formation of higher order supramolecular assemblies. Efforts pioneered by Lehn's concepts and work, aimed at emulating Nature's strategies by coalescing supramolecular chemistry and polymer science, have led to the noncovalent synthesis of polymers, i.e., "supramolecular polymers".[2]

Supramolecular polymers can be designed by choosing topological features and/or chemical surfaces of the interacting counterparts, capable of establishing a number of reversible noncovalent attractive intermolecular forces typical of host—guest and coordination chemistry. Because of the reversibility of noncovalent interactions, these materials are dynamic and capable of undergoing self-healing and adaptation processes,

[†] Università di Messina.
[‡] Present address: Università di Catania.
[§] Università di Catania.
[||] CNR, ICTP Catania.
[⊥] Tel Aviv University.

(1) Whitesides, G. M.; Simanek, E. E.; Mathias, J. P.; Seto, C. T.; Chin, D. N.; Mammen, M.; Gordon, D. M. *Acc. Chem. Res.* **1995**, *28*, 37–44.

10.1021/jo801202h CCC: $40.75
Published on Web 08/13/2008

which gives supramolecular polymers a major advantage over conventional, covalently bonded, polymers. The responsiveness to external stimuli may further imply a range of potential applications as smart/adaptive materials and devices.[3]

Among noncovalent interactions driving the formation of supramolecular polymers, multiple hydrogen bonding is one of the most favored,[4] owing to its biological relevance, directionality, and specificity.[5] Other typical recognition motifs employed in self-assembly processes include noncovalent forces as diverse as van der Waals,[6] hydrophilic/hydrophobic,[7] electrostatic interactions,[8] $\pi-\pi$ stacking,[9] metal−ligand coordination bonds,[10] crown ether/organic diammonium salt host−guest binding,[11] and nucleobase pair interactions.[12]

Although calixarenes are especially attractive building blocks in supramolecular chemistry for their availability and easy chemical alteration at both the wide and narrow rims, their potential in the construction of supramolecular polymers is relatively unexplored.[13] Rebek early reported the formation of polymeric capsules (polycaps)—via a seam of intermolecular hydrogen bonds—from the self-assembly in nonpolar media of tetraurea calix[4]arene dimers covalently linked at their lower rims.[14] Rudkevich described switchable supramolecular polycaps by introducing appropriate functions at the narrow rim of calix[4]arenes.[15] More recently, Fukazawa reported the formation of supramolecular nano networks from the self-assembly of a ditopic bisdouble-calix[5]arene and a dumbbell [60]-fullerene.[16]

In the quest for new molecules optimized for the formation of higher order architectures from smaller components, we have focused our attention on calix[5]arene-based homoditopic receptors as potential modules for the assembly of supramolecular structures by using iterative inclusion processes with complementary homoditopic connectors. We have already shown that *p-tert*-butylcalix[5]arenes in a fixed C_{5v} cone-like arrangement selectively form strong 1:1 inclusion complexes with linear alkylammonium ions[17] and discrete dimeric capsules in the presence of long-chained α,ω-alkanediyldiammonium ions, in which a single ditopic guest of appropriate length coordinates to a pair of calix[5]arene units.[18] The remarkable stability displayed by these host−guest complexes arises from the cooperative action of a number of noncovalent intermolecular forces, encompassing cation$-\pi$[19] (primary recognition motif) and C−H$\cdots\pi$[20] interactions, as well as hydrogen bonding of the deeply included tripodal ammonium ion with the ethereal oxygens.[21]

As a natural evolution of our ongoing work in this field, we have recently reported the formation of linear AB-type su-

(2) (a) Lehn, J.-M. *Supramolecular Chemistry - Concepts and Perspectives*; VCH: Weinheim, 1995. (b) Lehn, J.-M. In *Supramolecular science: Where it is and where it is going*; Ungaro, R., Dalcanale, E., Eds.; Kluwer: Dordrecht, The Netherlands, 1999; pp 287−304. (c) Brunsveld, L.; Folmer, B. J. B.; Meijer, E. W.; Sijbesma, R. P. *Chem. Rev.* **2001**, *101*, 4071–4097. (d) Lehn, J.-M. *Science* **2002**, *295*, 2400–2403. (e) Bosman, A. W.; Brunsveld, L.; Folmer, B. J. B.; Sijbesma, R. P.; Meijer, E. W. *Macromol. Symp.* **2003**, *201*, 143–154. (f) *Supramolecular Polymers*, 2nd ed.; Ciferri, A., Ed.; CRC Press: Boca Raton, FL, 2005. (g) Hofmeister, H.; Schubert, U. S. *Chem. Commun.* **2005**, 2423–2432. (h) Lehn, J.-M. *Prog. Polym. Sci.* **2005**, *30*, 814–831.

(3) (a) Lehn, J.-M. *Chem. Soc. Rev.* **2007**, *36*, 151–160. (b) Ulrich, S.; Lehn, J.-M. *Angew. Chem., Int. Ed.* **2008**, *47*, 2240–2243.

(4) (a) Lehn, J.-M. *Adv. Mater.* **1990**, *2*, 254–257. (b) Gulik-Krzywicki, T.; Fouquey, C.; Lehn, J.-M. *Proc. Natl. Acad. Sci. U.S.A.* **1993**, *90*, 163–167. (c) Lehn, J.-M. *Makromol. Chem., Macromol. Symp.* **1993**, *69*, 1–17. (d) Sijbesma, R. P.; Beijer, F. H.; Brunsveld, L.; Folmer, B. J. B.; Hirschberg, J. H. K. K.; Lange, R. F. M.; Lowe, J. K. L.; Meijer, E. W. *Science* **1997**, *278*, 1601–1604. (e) Hirschberg, J. H. K. K.; Brunsveld, L.; Ramzi, A.; Vekemans, J. A. J. M.; Sijbesma, R. P.; Meijer, E. W. *Nature* **2000**, *407*, 167–170. (f) Söntjens, S. H. M.; Sijbesma, R. P.; van Genderen, M. H. P.; Meijer, E. W. *Macromolecules* **2001**, *34*, 3815–3818. (g) Prins, L. J.; Reinhoudt, D. N.; Timmerman, P. *Angew. Chem., Int. Ed.* **2001**, *40*, 2382–2426. (h) Berl, V.; Schmutz, M.; Krische, M. J.; Khoury, R. G.; Lehn, J.-M. *Chem.—Eur. J.* **2002**, *8*, 1227–1244. (i) Cate, A. T.; Kooijman, H.; Spek, A. L.; Sijbesma, R. P.; Meijer, E. W. *J. Am. Chem. Soc.* **2004**, *126*, 3801–3808. (j) Mayer, M. F.; Nakashima, S.; Zimmerman, S. C. *Org. Lett.* **2005**, *7*, 3005–3008. (k) Park, T.; Todd, E. M.; Nakashima, S.; Zimmerman, S. C. *J. Am. Chem. Soc.* **2005**, *127*, 18133–18142. (l) Scherman, O. A.; Lightart, G. B. W. L.; Sijbesma, R. P.; Meijer, E. W. *Angew. Chem., Int. Ed.* **2006**, *45*, 2072–2076. (m) Scherman, O. A.; Lightart, G. B. W. L.; Ohkawa, H.; Sijbesma, R. P.; Meijer, E. W. *Proc. Natl. Acad. Sci. U.S.A.* **2006**, *103*, 11850–11855. (n) Ong, H. C.; Zimmerman, S. C. *Org. Lett.* **2006**, *8*, 1589–1592. (o) Park, T.; Zimmerman, S. C. *J. Am. Chem. Soc.* **2006**, *128*, 11582–11590. (p) Park, T.; Zimmerman, S. C. *J. Am. Chem. Soc.* **2006**, *128*, 13986–13987. (q) Park, T.; Zimmerman, S. C. *J. Am. Chem. Soc.* **2006**, *128*, 14236–14237.

(5) Jeffrey, G. A.; Saenger, W. *Hydrogen Bonding in Biological Structures*; Springer-Verlag: Berlin, 1991.

(6) (a) Hosseini, M. W.; De Cian, A. *Chem. Commun.* **1998**, 727–733. (b) Hosseini, M. W. *Acc. Chem. Res.* **2005**, *38*, 313–323.

(7) (a) Miyauchi, M.; Harada, A. *J. Am. Chem. Soc.* **2004**, *126*, 11418–11419. (b) Arnaud, A.; Belleney, J.; Boue, F.; Bouteiller, L.; Carrot, G.; Wintgens, W. *Angew. Chem., Int. Ed.* **2004**, *43*, 1718–1721. (c) Miyauchi, M.; Hoshino, T.; Yamaguchi, H.; Kamitori, S.; Harada, A. *J. Am. Chem. Soc.* **2005**, *127*, 2034–2035. (d) Miyauchi, M.; Takashima, Y.; Yamaguchi, H.; Harada, A. *J. Am. Chem. Soc.* **2005**, *127*, 2984–2989. (e) Hasegawa, Y.; Miyauchi, M.; Takashima, Y.; Yamaguchi, H.; Harada, A. *Macromolecules* **2005**, *38*, 3724–3730. (f) Ohga, K.; Takashima, Y.; Hirokazu, T.; Yoshinori, K.; Yamaguchi, H.; Harada, A. *Macromolecules* **2005**, *38*, 5897–5904. (g) Kuad, P.; Miyawaki, A.; Yoshinori, T.; Yamaguchi, H.; Harada, A. *J. Am. Chem. Soc.* **2007**, *129*, 12630–12631.

(8) (a) Purrello, R.; Gurrieri, S.; Lauceri, R. *Coord. Chem. Rev.* **1999**, *190*−*192*, 683–706. (b) Muraoka, M.; Kishimoto, N.; Yamashita, I. *Polym. Preprints* **2005**, *46*, 102–103.

(9) For the stacking of aromatic discotic molecules, see, for example, *Handbook of Liquid Crystals*; Demus, D., Goodby, J., Gray, G. W., Spiess, H. W., Vill, V., Eds.; Wiley-VCH: Weinheim, 1998; Vol. 2 B, and references therein.

(10) (a) Munakata, M.; Wu, L. P.; Kuroda-Sowa, T. *Bull. Chem. Soc. Jpn.* **1997**, *70*, 1727–1743. (b) Michelsen, U.; Hunter, C. A. *Angew. Chem., Int. Ed.* **2000**, *39*, 764–767. (c) Navarro, J. A. R.; Lippert, B. *Coord. Chem. Rev.* **2001**, *222*, 219–250. (d) Dai, J.-C.; Fu, Z.-Y.; Wu, X.-T. *Encyclopedia Nanosci. Nanotech.* **2004**, *10*, 247–266. (e) Schubert, U. S.; Eschbaumer, C. *Angew. Chem., Int. Ed.* **2002**, *41*, 2892–2926. (f) Chen, C.-C.; Dormidontova, E. E. *J. Am. Chem. Soc.* **2004**, *126*, 14972–14978. (g) Dobrawa, R.; Wuerthner, F. *J. Polym. Sci., Part A: Polym. Chem.* **2005**, *43*, 4981–4995. (h) Carlucci, L.; Ciani, G.; Proserpio, D. M.; Porta, F. *CrystEngComm* **2006**, *8*, 696–706.

(11) (a) Yamaguchi, N.; Nagvekar, D. S.; Gibson, H. W. *Angew. Chem., Int. Ed.* **1998**, *37*, 2361–2364. (b) Yamaguchi, N.; Gibson, H. W. *Angew. Chem., Int. Ed.* **1999**, *38*, 143–147. (c) Gibson, H. W.; Yamaguchi, N.; Jones, J. W. *J. Am. Chem. Soc.* **2003**, *125*, 3522–3533. (d) Huang, F.; Gibson, H. W. *Chem. Commun.* **2005**, 1696–1698. (e) Huang, F.; Nagvekar, D. S.; Zhou, X.; Gibson, H. W. *Macromolecules* **2007**, *40*, 3561–3567.

(12) (a) Sivakova, S.; Wu, J.; Campo, C. J.; Mather, P. T.; Rowan, S. J. *Chem.—Eur. J.* **2006**, *12*, 446–456. (b) Burke, K. A.; Sivakova, S.; McKenzie, B. M.; Mather, P. T.; Rowan, S. J. *J. Polym. Sci., Part A: Polym. Chem.* **2006**, *44*, 5049–5059.

(13) (a) Böhmer, V. *Angew. Chem., Int. Ed.* **1995**, *34*, 713–745. (b) Ikeda, A.; Shinkai, S. *Chem. Rev.* **1997**, *97*, 1713–1734. (c) Gutsche, C. D. *Calixarenes Revisited (Monographs in Supramolecular Chemistry)*; Stoddart, J. F., Ed.; The Royal Society of Chemistry: Cambridge, 1998; Vol. 6. (d) *Calixarenes 2001*; Asfari, Z., Böhmer, V., Harrowfield, J., Vicens, J., Eds.; Kluwer Academic Publishers: Dordrecht, 2001.

(14) (a) Shimizu, K. D.; Rebek, J., Jr. *Proc. Natl. Acad. Sci. U.S.A.* **1995**, *92*, 12403–12407. (b) Castellano, R. K.; Rudkevich, D. M.; Rebek, J., Jr. *Proc. Natl. Acad. Sci. U.S.A.* **1997**, *94*, 7132–7137. (c) Castellano, R. K.; Rebek, J., Jr. *J. Am. Chem. Soc.* **1998**, *120*, 3657–3663. (d) Castellano, R. K.; Nuckolls, C.; Eichhorn, S. H.; Wood, M. R.; Lovingen, A. J.; Rebek, J., Jr. *Angew. Chem., Int. Ed.* **1999**, *38*, 2603–2606. (e) Castellano, R. K.; Clark, R.; Craig, S. L.; Nuckolls, C.; Rebek, J., Jr. *Proc. Natl. Acad. Sci. U.S.A.* **2000**, *97*, 12418–12421.

(15) (a) Xu, H.; Stampp, S. P.; Rudkevich, D. M. *Org. Lett.* **2003**, *5*, 4583–4586. (b) Xu, H.; Hampe, E. M.; Rudkevich, D. M. *Chem. Commun.* **2003**, 2828–2829. (c) Xu, H.; Rudkevich, D. M. *Chem.—Eur. J.* **2004**, *10*, 5432–5442.

(16) Haino, T.; Matsumoto, Y.; Fukazawa, Y. *J. Am. Chem. Soc.* **2005**, *127*, 8936–8937.

(17) (a) Arnaud-Neu, F.; Fuangswasdi, S.; Notti, A.; Pappalardo, S.; Parisi, M. F. *Angew. Chem., Int. Ed.* **1998**, *37*, 112–114. (b) Ferguson, G.; Notti, A.; Pappalardo, S.; Parisi, M. F.; Spek, A. L. *Tetrahedron Lett.* **1998**, *39*, 1969–1972. (c) Notti, A.; Parisi, M. F.; Pappalardo, S. In *Calixarene 2001*; Asfari, Z., Böhmer, V., Harrowfield, J., Vicens, J., Eds.; Kluwer Academic: Dordrecht, 2001; pp 54−70. (d) De Salvo, G.; Gattuso, G.; Notti, A.; Parisi, M. F.; Pappalardo, S. *J. Org. Chem.* **2002**, *67*, 684–692.

(18) Garozzo, D.; Gattuso, G.; Kohnke, F. H.; Malvagna, P.; Notti, A.; Occhipinti, S.; Pappalardo, S.; Parisi, M. F.; Pisagatti, I. *Tetrahedron Lett.* **2002**, *43*, 7663–7667.

(19) Ma, J. C.; Dougherty, D. A. *Chem. Rev.* **1997**, *97*, 1303–1324.

(20) (a) Nishio, M.; Hirota, H.; Umezawa, Y. *The CH/π Interaction. Evidence, Nature and Consequences*; Wiley-VCH: New York, 1998. (b) Nishio, M. *CrystEngComm* **2004**, *6*, 130–158.

pramolecular oligomers from the proton-driven self-assembly of a calix[5]arene derivative bearing a 12-aminododecyl pendant group on the lower rim (AB-type[22] host−guest conjugates) via iterative intermolecular inclusion events.[23] Furthermore, the guest-induced capsular assembly[18] of calix[5]arenes and α,ω-alkanediyldiammonium ions has suggested that, by covalently linking two such calix[5]arenes at their lower rims with an appropriate spacer, their cores diverge and inclusion of suitable α,ω-alkanediyldiammonium ions should eventually result in the formation of (poly)capsular assemblies. In this paper, we report on the synthesis of homoditopic building blocks *p*-, *m*-, and *o*-**1**, featuring two π-rich cone-like calix[5]arene cavities (assembling cores) connected by a rigid *p*-, *m*-, and *o*-xylyl spacer in a centrosymmetric divergent arrangement and the study of their self-assembly dynamics with the complementary α,ω-alkanediyldiammonium ions as a function of the length of the connectors, the geometry of the spacer, as well as the concentration and/or molar ratio between the two components.[24]

Results and Discussion

Synthesis. Bis-calix[5]arenes **1** in a fixed cone conformation were obtained by a two-step synthesis involving the tail-to-tail bridging of *p-tert*-butylcalix[5]arene **2**[25] with isomeric α,α′-dibromoxylene spacers and CsF in dry DMF at room temperature to produce octols **3**, followed by the exhaustive alkylation of the residual hydroxyl groups with an excess of 4-methylpentyl tosylate[26] and K_2CO_3 in refluxing acetonitrile (Scheme 1). The structures of homoditopic bis-calix[5]arenes *p*-, *m*-, and *o*-**1** were assigned on the basis of NMR and ESI-MS evidence and single-crystal X-ray analysis of *p*-**1**.[24]

Mass Spectroscopy. The electrospray ionization (ESI)[27] is one of the softest ionization methods currently used for the gas-phase study of host−guest complexation[28] and supramolecular assembly[29] by mass spectrometry. It readily allows the mass spectrometric detection of self-assembling encapsulation complexes,[30] hydrogen-bonding assemblies,[31] very large pyrogallarene and resorcinarene hexameric capsules,[32] and self-assembling dendrimers.[33] We have used electrospray ionization mass spectrometry (ESI-MS) for the gas-phase characterization of the supramolecular assemblies generated from the modular interaction of homoditopic bis-calix[5]arenes *p*-, *m*-, and *o*-**1** and α,ω-alkanediyldiammonium dipicrate guest (**G**) salts $\mathbf{C_8}-\mathbf{C_{12}}$·2Pic (**1**:**G** molar ratio 1:1, 10 μM in $CHCl_3/CH_3OH$ 1:1, v/v). Diammonium ions not only act as supramolecular components but also provide the ion labels necessary for the ESI-MS characterization of the assemblies.

SCHEME 1. Synthesis of Bis-calix[5]arenes 1

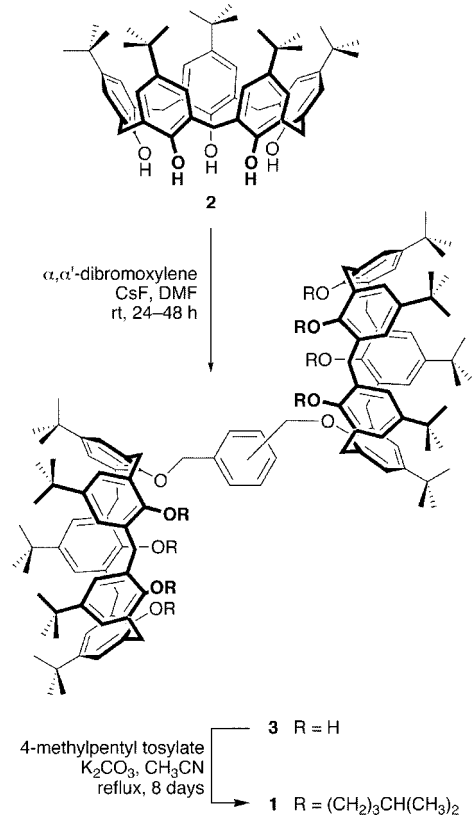

The ESI mass spectral behavior of the various **1/G** combinations is quite uniform, and a typical mass spectrum, relative to the *o*-$\mathbf{1/C_{10}}$ pair, is shown in Figure S1a (see the Supporting Information).

The spectrum is dominated by prominent ion peaks at *m/z* 2570.2 ($[\mathbf{C_{10}}\subset o\text{-}\mathbf{1} - H]^+$) and 1285.7 ($[\mathbf{C_{10}}\subset o\text{-}\mathbf{1}]^{2+}$, base peak), corresponding to the singly or doubly charged 1:1 *o*-$\mathbf{1/C_{10}}$ *endo*-cavity inclusion complex (type A, Figure 1). The third most intense ion peak at *m/z* 2484.2 ($[o\text{-}\mathbf{1}\supset\mathbf{C_{10}}\subset o\text{-}\mathbf{1}]^{2+}$) provides clear evidence for the formation of a doubly charged 2:1 *o*-$\mathbf{1/C_{10}}$ capsular assembly (type C, Figure 1). Apart from other intense ion peaks at *m/z* 2436.2 ($[K\subset o\text{-}\mathbf{1}]^+$), 2419.2 ($[Na\subset o\text{-}\mathbf{1}]^+$), and 2414.3 ($[NH_4\subset o\text{-}\mathbf{1}]^+$), associated with the formation of bis-calix[5]arene 1:1 complexes with adventitious alkali metal ions, the spectrum shows a moderately intense but diagnostically important ion peak at *m/z* 1371.7 ($[\mathbf{C_{10}}\subset o\text{-}\mathbf{1}\supset\mathbf{C_{10}} - 2H]^{2+}$), corresponding to the 1:2 *o*-$\mathbf{1/C_{10}}$ bis-*endo*-cavity inclusion complex (type B, Figure 1), and triply charged ion peaks of

(21) N−H···O hydrogen bonding has recently been detected in the solid state structure of the *n*-butylammonium/5,11,17,23,29-pentakis(1,1-dimethylethyl)-31,32,33,34,35-penta(4-methylpentyloxy)calix[5]arene 1:1 *endo*-cavity inclusion complex; Pilati, T. *et. al.*, manuscript in preparation.

(22) (a) Jiménez, M. C.; Dietrich-Buchecker, C.; Sauvage, J. P.; De Cian, A. *Angew. Chem., Int. Ed.* **2000**, *39*, 1295–1298. (b) Hoshino, T.; Miyauchi, M.; Kawaguchi, Y.; Yamaguchi, H.; Harada, A. *J. Am. Chem. Soc.* **2002**, *124*, 9876–9877.

(23) (a) Pappalardo, S.; Villari, V.; Slovak, S.; Cohen, Y.; Gattuso, G.; Notti, A.; Pappalardo, A.; Pisagatti, I.; Parisi, M. F. *Chem.−Eur. J.* **2007**, *13*, 8164–8173. (b) For similar observations on a pyridinium-containing calix[4]arene, see: Ishihara, S.; Takeoka, S. *Tetrahedron Lett.* **2006**, *47*, 181–184.

(24) For a preliminary account of this research, see: Garozzo, D.; Gattuso, G.; Kohnke, F. H.; Notti, A.; Pappalardo, S.; Parisi, M. F.; Pisagatti, I.; White, A. J. P.; Williams, D. J. *Org. Lett.* **2003**, *5*, 4025–4028.

(25) Stewart, D. R.; Gutsche, D. C. *Org. Prep. Proc. Int.* **1993**, *25*, 137–139.

(26) Prestwich, G. D.; Graham, S. McG.; Kuo, J.-W.; Vogt, R. G. *J. Am. Chem. Soc.* **1989**, *111*, 636–642.

(27) (a) Fenn, J. B.; Mann, M.; Meng, C. K.; Wong, S. F.; Whitehouse, C. M. *Mass Spectrom. Rev.* **1990**, *9*, 37–70. (b) Kebarle, P.; Tang, L. *Anal. Chem.* **1993**, *65*, 972A–986A. (c) Gaskell, S. J. *J. Mass Spectrom.* **1997**, *32*, 677–688.

(28) Sherman, C. L.; Brodbelt, J. S. *Anal. Chem.* **2003**, *75*, 1828–1836.

(29) (a) Schalley, C. A. *Mass Spectrom. Rev.* **2001**, *20*, 253–309. (b) Baytekin, B.; Baytekin, H. T.; Schalley, C. A. *Org. Biomol. Chem.* **2006**, *4*, 2825–2841.

(30) (a) Schalley, C. A.; Martín, T.; Obst, U.; Rebek, J., Jr. *J. Am. Chem. Soc.* **1999**, *121*, 2133–2138. (b) Schalley, C. A.; Castellano, R. K.; Brody, M. S.; Rudkevich, D. M.; Siuzdak, G.; Rebek, J., Jr. *J. Am. Chem. Soc.* **1999**, *121*, 4568–4579. (c) Lützen, A.; Renslo, A. R.; Schalley, C. A.; O'Leary, B. M.; Rebek, J., Jr. *J. Am. Chem. Soc.* **1999**, *121*, 7455–7456. (d) Mansikkamäki, H.; Nissinen, M.; Schalley, C. A.; Rissanen, K. *New J. Chem.* **2003**, *27*, 88–97. (e) Garozzo, D.; Gattuso, G.; Notti, A.; Pappalardo, A.; Pappalardo, S.; Parisi, M. F.; Perez, M.; Pisagatti, I. *Angew. Chem., Int. Ed.* **2005**, *44*, 4892–4896.

(31) Letzel, M. C.; Decker, B.; Rozhenko, A. B.; Schoeller, W. W.; Mattay, J. *J. Am. Chem. Soc.* **2004**, *126*, 9669–9674.

(32) Beyeh, N. K.; Kogej, M.; Åhman, A.; Rissanen, K.; Schalley, C. A. *Angew. Chem., Int. Ed.* **2006**, *45*, 5214–5218.

(33) Schalley, C. A.; Baytekin, B.; Baytekin, H. T.; Engeser, M.; Felder, T.; Rang, A. *J. Phys. Org. Chem.* **2006**, *19*, 479–490.

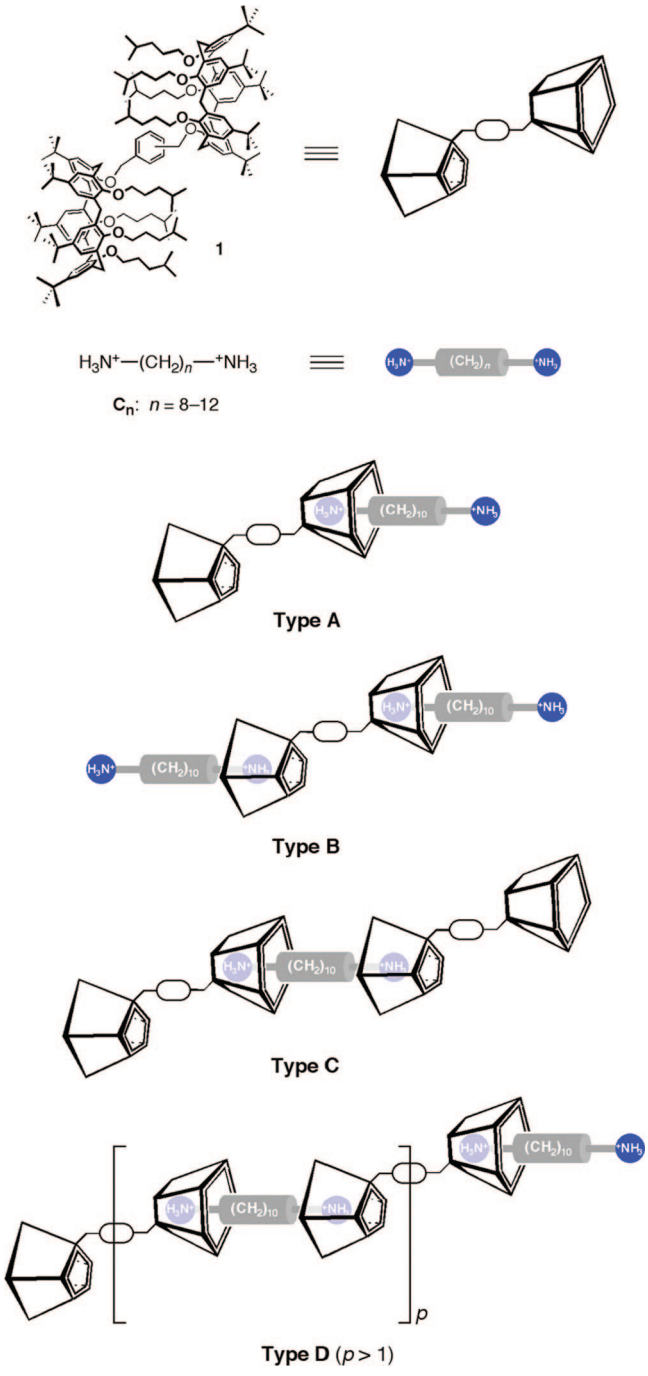

FIGURE 1. Schematic representation of the assemblies derived from the binding of alkanediyldiammonium ions $\mathbf{C}_n$ to bis-calix[5]arenes **1**.

much lower intensity at *m*/*z* 1790.0 ([*o*-**1**⊃$\mathbf{C_{10}}$⊂*o*-**1**⊃$\mathbf{C_{10}}$ + Pic]$^{3+}$) and 1713.6 ([*o*-**1**⊃$\mathbf{C_{10}}$⊂*o*-**1**⊃$\mathbf{C_{10}}$ – H]$^{3+}$), consistent with 2:2 capsular assemblies of the modular *o*-**1**/$\mathbf{C_{10}}$ components (type D for $p = 1$, Figure 1).[34] The most relevant ion peaks in the ESI mass spectra of the 15 couples of modular components, and their relative assignments are collected in Table S1 (see the Supporting Information).

The binding selectivities of diastereoisomers *p*-, *m*-, and *o*-**1** toward diammonium ions $\mathbf{C_8}$−$\mathbf{C_{12}}$ were estimated in competitive complexation experiments by measuring the ion intensities of the relevant complexes observed after analyzing solutions of **1** in the presence of equimolar mixtures of the five diammonium picrate salts (**1**:$\mathbf{C_8}$:$\mathbf{C_9}$:$\mathbf{C_{10}}$:$\mathbf{C_{11}}$:$\mathbf{C_{12}}$, 10 μM in each component, $CHCl_3/CH_3OH$ 2:1, v/v). A typical mass spectrum, relevant to the *o*-**1**/$\mathbf{C_8}$–$\mathbf{C_{12}}$ experiment, is reported in Figure S1b (Supporting Information). The spectrum displays collections of ion peaks that allow us to easily estimate the intrinsic stabilities of the various types of complexes/assemblies by direct comparison of their intensities within each family. The spectrum is dominated by ion peaks due to the 1:1 *endo*-cavity complex, which can show up both as singly [**G**⊂*o*-**1** − H]$^+$ and doubly charged [**G**⊂*o*-**1**]$^{2+}$ ions. The intensities of the former ions indicate a slight preference of receptor *o*-**1** for $\mathbf{C_{10}}$ and $\mathbf{C_{11}}$ diammonium ions, while those of the latter increase by increasing the end-to-end distance between the two ammonium groups (i.e., $\mathbf{C_8}$ < $\mathbf{C_9}$ < $\mathbf{C_{10}}$ < $\mathbf{C_{11}}$ < $\mathbf{C_{12}}$), presumably as a result of a better minimization of the electrostatic repulsion between the two positive charges. The ion [$\mathbf{C_{12}}$⊂*o*-**1**]$^{2+}$ (*m*/*z* 1299.6) reaches the base peak in the spectrum in all cases under study.

The aptitude of the longer alkanediyldiammonium ions to induce capsular assemblies with homoditopic bis-calix[5]arene *o*-**1** is evidenced by the presence of the doubly charged [*o*-**1**⊃$\mathbf{C}_n$⊂*o*-**1**]$^{2+}$ ion peaks in the 2470−2498 mass range. The binding selectivity follows the order $\mathbf{C_{10}}$ > $\mathbf{C_{12}}$ > $\mathbf{C_{11}}$ ≫ $\mathbf{C_9}$ > $\mathbf{C_8}$ with *m*-**1** and *p*-**1**, and $\mathbf{C_{12}}$ > $\mathbf{C_{10}}$ > $\mathbf{C_{11}}$ ≫ $\mathbf{C_9}$ > $\mathbf{C_8}$ with *o*-**1**. On the other hand, the formation of the 1:2 (**1**:**G**) complexes is corroborated by a collection of doubly charged ion peaks of moderate intensities in the mass range 1344−1399 ([$\mathbf{C}_n$⊂*o*-**1**⊃$\mathbf{C}_m$ − 2H]$^{2+}$, $n = m$ and/or $n > m$),[35] the most intense ion pertaining to the mixed $\mathbf{C_{10}}$/$\mathbf{C_{11}}$ 1:2 bis-*endo*-cavity complex. Furthermore, the presence in the spectra of two more families of low intensity triply charged ion peaks in the 1694−1732 and 1771−1808 mass ranges, corresponding to [*o*-**1**⊃$\mathbf{C}_n$⊂*o*-**1**⊃$\mathbf{C}_m$ − H]$^{3+}$ and [*o*-**1**⊃$\mathbf{C}_n$⊂*o*-**1**⊃$\mathbf{C}_m$ + Pic]$^{3+}$, respectively, provide evidence for the formation of the 2:2 (*o*-**1**:**G**) assemblies.

NMR Titration/Dilution Studies. Extensive NMR investigations were carried out to elucidate the self-assembly dynamics of homoditopic bis-calix[5]arene hosts *p*-, *m*-, and *o*-**1** and complementary α,ω-alkanediyldiammonium guests in solution. Taking advantage of our earlier observations on single-[18] and double-cavity[24] calix[5]arene hosts and the ESI-MS investigations discussed above, NMR studies were focused on 1,10-decanediyldiammonium dipicrate $\mathbf{C_{10}}$·2Pic, as the length of this dication was judged to be ideal for the formation of a variety of supramolecular species. As expected, the **1**/$\mathbf{C_{10}}$ complementary pairs showed dynamic behavior, responding to changes in concentration and/or in molar ratio by rearranging into different assemblies. According to an inevitably simplified overall picture, which of course does not account for all the possible coexisting species, four distinct species were identified: a 1:1 *endo*-cavity assembly $\mathbf{C_{10}}$⊂**1**, a 1:2 bis-*endo*-cavity assembly $\mathbf{C_{10}}$⊂**1**⊃$\mathbf{C_{10}}$, a monocapsular assembly **1**⊃$\mathbf{C_{10}}$⊂**1**, and a polycapsular assembly **1**⊃($\mathbf{C_{10}}$⊂**1**)$_p$⊃$\mathbf{C_{10}}$ (referred to as types A−D, respectively, in Figure 1).

^{1}H NMR spectroscopy proved to be an excellent tool to assess the structural features of these types of assemblies and monitor the dynamics of formation/dissociation. Host and guest components were found to possess diagnostic probe signals (see Figure 2) undergoing (in slow exchange regime on the NMR

(34) Molecular modeling, as well as inspection of CPK models, rule out the formation of cyclic [**1**⊃$\mathbf{C_{10}}$⊂**1**⊃$\mathbf{C_{10}}$⊂] species. Self-assembly of such species would require a spacer longer than a xylyl moiety, and/or a guest much longer than a decanediyldiammonium (or dodecanediyldiammonium) dication.

(35) The subscripts $n = m$ or $n > m$ refer to diammonium guests of the same or different length, respectively.

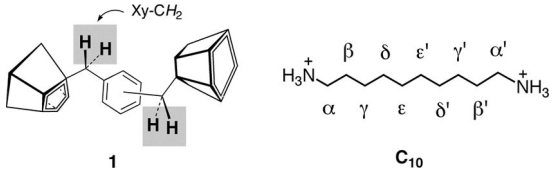

FIGURE 2. Probe groups used for ^{1}H NMR structural elucidation according to molecular symmetry within the assembled supramolecular species.

SCHEME 2. Schematic Representation of the Cyclic and Reversible Process Featuring the Self-Assembly Dynamics of Modular Homoditopic Bis-calix[5]arenes 1 and C_{10} Components

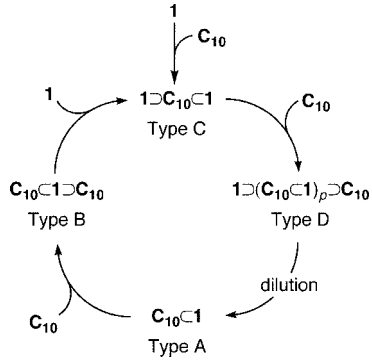

time scale) substantial and distinctive chemical shift changes upon self-assembly as a function of the symmetry elements present within a given assembled species.

Specifically, the peaks belonging to the benzylic hydrogen atoms of the xylyl spacer (Xy-CH_2) of bis-calixarenes **1** may resonate either as one singlet, when both cavities are empty (free host) or when they are both hosting one end of $\mathbf{C_{10}}$ (i.e., type B or core of type D), or as two distinct singlets, when only one of the two cavities is filled by a diammonium ion (i.e., type A or type C). Complex formation does induce symmetrization/desymmetrization of the guest as well. Accordingly, when the two methylene groups at the far ends of $\mathbf{C_{10}}$ (α-CH_2 and α′-CH_2) are both cavity-included (by any of the three isomeric hosts under study) they are equivalent and—as a result of the shielding induced by the aromatic walls of the calixarene moieties—resonate as a high-field broad singlet at $\delta = -1.38 \pm 0.02$ ppm (i.e., type C or type D), whereas they appear as two distinct resonances when only half of the dication is embedded into the cavity of a calixarene subunit (i.e., type A or B).[18] In the latter case, the included α-CH_2[36] signal resonates at $\delta = -1.27 \pm 0.01$ ppm whereas the α′-CH_2,[36] at the opposite end of the dication, appears as a triplet at $\delta = 2.86 \pm 0.05$ ppm. ^{1}H NMR peak assignments for selected probe groups of modular pairs of **1** and $\mathbf{C_{10}}$ components are collected together in Table S2 (see the Supporting Information).

In order to identify the different types of assemblies, a simple series of ^{1}H NMR experiments was devised, so as to induce—in a cyclic fashion (Scheme 2)—a progressive evolution of the self-assembled species upon variation of the host/guest molar ratio and/or concentration.

When $\mathbf{C_{10}}$ (0.25 equiv) was added to a 50 mM $CDCl_3/CD_3OD$ (9:1, v/v) solution of *p*-**1** (Figure S2, trace a, see the Supporting Information), so as to reach a 4:1 host/guest ratio, the spectrum (Figure S2, trace b, see the Supporting Information) revealed the formation of a monocapsular type C assembly as demonstrated by the presence of two equally intense singlets for the *p*-Xy-CH_2 ($\delta = 4.81$ and 4.92 ppm, 2H each), along with free bis-calixarene *p*-**1** (*p*-Xy-CH_2, $\delta = 4.77$ ppm). In keeping with the formation of a type C assembly, host desymmetrization (signal doubling) is accompanied by the presence—in the high-field region (−2.0 to 0.3 ppm)—of a single set of peaks, for the α- to ϵ-CH_2 and the symmetry-related α′- to ϵ′-CH_2 groups of the guest, shielded by the π-rich cavities of two host molecules arranged in a monocapsular fashion. Note that no resonances compatible with the presence of either free guest (α-CH_2 ≡ α′-CH_2) or type A and B assemblies (*exo*-cavity α′-CH_2) are observed in the diagnostic $\delta = 2.86 \pm 0.05$ ppm region (see below).

Further addition of 0.75 equiv of $\mathbf{C_{10}}$ to the above solution ([*p*-**1**] = [$\mathbf{C_{10}}$] = 50 mM), promoted the formation of polycapsular assemblies of type D (both host and guest components are now symmetric, with the exception of the two "end-cavities"), as deduced by the presence of a broad singlet for the pair of equivalent *p*-Xy-CH_2 groups of the host ($\delta = 4.92$ ppm, 4H) and the persistence and broadening of the signals belonging to the α- to α′-CH_2 groups of $\mathbf{C_{10}}$ in the −2.0 to 0.3 ppm high-field region (Figure S2, trace c, see the Supporting Information). The low intensity peaks (4.81 ppm (singlet) and 2.91 ppm (triplet) as well as the two humps located at −1.26 and −0.18 ppm) present in this spectrum are assigned either to the end-groups (empty cavity of the host on one side and one end of $\mathbf{C_{10}}$ filling the cavity on the other) of type D assemblies or the incipient cleavage of such assemblies leading to the formation of a small fraction of the 1:1 type A complex (see below). Both type A as well as the "end-cavities" of type D assemblies are indeed expected to provide similar ^{1}H NMR patterns deriving from the desymmetrization (one cavity empty and one full) of both host and guest.

Dilution of the equimolar 50 mM solution of the two components down to 1 mM leads to the disruption of the polycapsular assemblies and mainly yields the 1:1 *endo*-cavity complex (type A). Contrary to the monocapsular assembly (type C), the formation of the type A assembly results in the desymmetrization of both host and guest and, as a result, the pertinent ^{1}H NMR spectrum (Figure S2, trace d, see the Supporting Information) shows the reappearance of two singlets for the two nonequivalent *p*-Xy-CH_2 groups ($\delta = 4.81$ and 4.92 ppm, 2H each) and the presence of a triplet centered at $\delta = 2.82$ ppm (α′-CH_2) together with an all new set of *endo*-cavity included methylene peaks (α- to ϵ-CH_2) in the −1.96 to 0.59 ppm region. The slightly downfield shift of the latter with respect to the one observed for the type C and D assemblies can be attributed to the reduced shielding effect from only one rather than two aromatic cavities. The spectrum also displays a singlet at $\delta = 4.77$ ppm and a triplet (overlapping with the one discussed above, $\delta = 2.84$ ppm) assigned to the free host and guest, respectively; as well as a low intensity set of *endo*-cavity included methylene peaks (α- to ϵ-CH_2) likely due to the concomitant persistence of low percentages of type D and/or C assemblies.

Upon addition of an excess of $\mathbf{C_{10}}$ (up to 1:5 host/guest ratio) the system evolves to the 1:2 bis-*endo*-cavity type B complex (Figure S2, trace e, see the Supporting Information). Under these conditions, the xylyl spacer of *p*-**1** becomes symmetric once again because of the filling of both cavities (*p*-Xy-CH_2 δ =

(36) For the sake of convenience, in the cases of type A and B inclusion complexes, we arbitrarily designate the methylene end-group of $\mathbf{C_{10}}$ located inside and outside the calixarene cavity as α-CH_2 and α′-CH_2, respectively.

TABLE 1. Diffusion Coefficients (D) of the Assemblies Formed in $CDCl_3/CD_3OD$ (2:1, v/v; 298 K) at Different *p*-1 (10 mM)/C_8 Molar Ratios

	D ($\times 10^{-5}$ cm^2 s^{-1})				
	host/guest molar ratio				
peak (ppm) (assignment)	1:0.25	1:0.5	1:1	1:2	1:4
−1.17 (α-CH_2, type A or B)	0.27 ± 0.01	0.26 ± 0.01	0.27 ± 0.01	0.25 ± 0.01	0.23 ± 0.01
2.72−2.76 (α′-CH_2, type A or B)	0.28 ± 0.01	0.28 ± 0.01	0.27 ± 0.01	0.25 ± 0.01	0.23 ± 0.01
2.89 (α-CH_2 ≡ α′-CH_2, free **C_8**)			0.44 ± 0.01	0.44 ± 0.01	0.42 ± 0.01
4.80 (Xy-CH_2, free *p*-**1**)	0.32 ± 0.01	0.32 ± 0.01			
4.84 (Xy-CH_2, type A)	0.31 ± 0.01	0.29 ± 0.01	0.27 ± 0.01	0.26 ± 0.01	
4.98 (Xy-CH_2, type A or B)	0.28 ± 0.01	0.28 ± 0.01	0.26 ± 0.01	0.24 ± 0.01	0.22 ± 0.01
8.80 (picrate)	0.59 ± 0.02	0.54 ± 0.01	0.49 ± 0.01	0.47 ± 0.01	0.46 ± 0.01
3.30 (residual CHD_2OD)	1.39 ± 0.03	1.20 ± 0.02	1.38 ± 0.01	1.36 ± 0.02	1.23 ± 0.02

4.92 ppm), whereas the guest remains desymmetrized and shows the typical pattern of a half-included diammonium ion, identical to the one observed for type A complex. Lastly, in a final double check experiment to confirm the fully dynamic self-assembly nature of the *p*-**1**/**C_{10}** complementary pair, it was shown that a concentration increase of *p*-**1** (from 1 to 20 mM) in the above solution of type B complex ([*p*-**1**] = 1 mM, [**C_{10}**] = 5 mM) to reestablish a 4:1 ratio was able to make the system revert to the initial monocapsular type C assembly (spectrum not shown).

Dynamic behavior and equivalent type A−D assembly formation were also observed when the other two isomeric hosts *m*- and *o*-**1** were subjected to analogous titration/dilution NMR experiments in the presence of **C_{10}** (see the Supporting Information, Figures S3 and S4).

NMR Diffusion Studies. To shed further light on the dynamics and modes of assembly between bis-calixarenes **1** and α,ω-alkanediyldiammonium dipicrates **C_n**·2Pic and validate at the same time the ^{1}H NMR results with a size-sensitive technique, extensive diffusion NMR studies[37] were undertaken. The diffusion NMR technique provides a means to simultaneously obtain the diffusion coefficients (D) of all the different supramolecular species coexisting in solution, as long as they display distinct and not superimposed peaks.[38] In recent years, diffusion studies have been of key relevance in assessing the nature of supramolecular assemblies in solution, including cyclodextrins,[7g,38c,39] peptides and proteins,[40] helicates,[41] resorcarene capsules and congeners,[42] isoG complexes,[43] cucurbiturils,[44] calixarene assemblies,[45] as well as calix[5]arene-based supramolecular polymers.[23a]

Following a preliminary screening (see the Supporting Information, Table S3), titration experiments of *p*-**1** with **C_n** were carried out in $CDCl_3/CD_3OD$ (2:1, v/v) solution at a fixed 10 mM host concentration, to ensure complete solubility of the salt guest present in excess at low host/guest ratio (e.g., 1:4) and avoid diffusion coefficients being influenced by viscosity effects. Gradual addition of **C_8**·2Pic (0.25−4.0 equiv) to a 10 mM solution of *p*-**1**, monitored by following the D values of the probe resonances associated with the host and guest Xy-CH_2, α-CH_2,[36] and α′-CH_2[36] groups, revealed the exclusive formation of type A and B assemblies in the presence of [**C_8**] ≤ 10 mM and [**C_8**] > 10 mM, respectively (Table 1).

The D values of the 1:1 *endo*-cavity complex (type A: D = (0.26−0.28 ± 0.01) × 10^{-5} cm^2 s^{-1}) are in between those measured for the free host (D = (0.32 ± 0.01) × 10^{-5} cm^2 s^{-1}) and the 1:2 bis-*endo*-cavity complex (type B: D = (0.22−0.25 ± 0.01) × 10^{-5} cm^2 s^{-1}). Binding of either one or two guest molecules to *p*-**1** (i.e., types A and B, respectively) increases the molar mass and, as a result, the diffusion coefficients of the new species decrease. This result confirms that **C_8** is not long enough to make two *p*-**1** units join in a capsular arrangement.

On the other hand, when the same titration experiments were repeated with the longer **C_{10}** guest, a wider range of assemblies was observed that fully matched the ^{1}H NMR observation. In this case, upon addition of **C_{10}** (0.25−0.5 equiv) to *p*-**1**, the diffusion coefficients associated with the α- to ε-CH_2 and the symmetry-related α′- to ε′-CH_2 groups of the host/guest complementary pair were found to be significantly lower (D = (0.18−0.20 ± 0.01) × 10^{-5} cm^2 s^{-1}) than those measured for the free host (D = (0.32 ± 0.01) × 10^{-5} cm^2 s^{-1}) and at the same time smaller than those observed in the case of **C_8** (D = (0.26−0.28 ± 0.01) × 10^{-5} cm^2 s^{-1}) at the same host/guest ratio (Table 2, see also Table S4 in the Supporting Information).

This trend was then rationalized with the formation of monocapsular assemblies (type C) with the "external cavities" empty (absence of the diagnostic α′-CH_2 resonance at δ = 2.86 ± 0.05 ppm). As titration proceeded, further addition of the guest first yielded polycapsular assemblies (type D, p = 2), as the host/guest ratio progressively changed from 1:0.67 to 1:1, followed by type B complexes when it reached the final 1:4 ratio. In agreement with this overall picture, the diffusion coefficients—calculated from the stack plots of the signal decay as a function of the gradient strength (G)—for the probe α-CH_2 peaks of the guest (δ = −1.30 and −1.19 ppm) were initially found to be (0.18−0.20 ± 0.01) × 10^{-5} cm^2 s^{-1} in the presence of the monocapsular assembly (*p*-**1**:**C_{10}** = 1:0.25−1:0.5), they then decreased to (0.14−0.15 ± 0.01) × 10^{-5} cm^2 s^{-1} upon polycapsular formation (*p*-**1**:**C_{10}** = 1:0.67−1:1), and finally grew again ((0.21−0.23 ± 0.01) × 10^{-5} cm^2 s^{-1}) when, in the

(37) For reviews on the application of diffusion NMR in chemical systems, see: (a) Stilbs, P. *Prog. NMR Spectrosc.* **1987**, *19*, 1–45. (b) Johnson, C. S., Jr. *Prog. NMR Spectrosc.* **1999**, *34*, 203–256.

(38) For a recent overview on the applications of diffusion NMR in supramolecular chemistry see Cohen, Y.; Avram, L.; Frish, L. *Angew. Chem., Int. Ed.* **2005**, *44*, 520–554. (a) For a few general examples of the applications of diffusion NMR in supramolecular chemistry, see Mayzel, O.; Cohen, Y. *J. Chem. Soc., Chem. Commun.* **1994**, 1901–1902. (b) Mayzel, O.; Aleksiuk, O.; Grynszpan, F.; Biali, S. E.; Cohen, Y. *J. Chem. Soc., Chem. Commun.* **1995**, 1183–1184. (c) Gafni, A.; Cohen, Y. *J. Org. Chem.* **1997**, *62*, 120–125. (d) Frish, L.; Matthews, S. E.; Böhmer, V.; Cohen, Y. *J. Chem. Soc., Perkin Trans. 2* **1999**, 669–671. (e) Tominaga, M.; Suzuki, K.; Kawano, M.; Kusukawa, T.; Ozeki, T.; Sakamoto, S.; Yamaguchi, K.; Fujita, M. *Angew. Chem., Int. Ed.* **2004**, *43*, 5621–5625. (f) Kuhnert, N.; Le-Gresley, A. *Org. Biomol. Chem.* **2005**, *3*, 2175–2182.

(39) (a) Cameron, K. S.; Fielding, L. *J. Org. Chem.* **2001**, *66*, 6891–6895. (b) Cabaleiro-Lago, C.; Nilsson, M.; Soederman, O. *Langmuir* **2005**, *21*, 11637–11644. (c) Valente, A. J. M.; Nilsson, M.; Soederman, O. *J. Colloid Interface Sci.* **2005**, *281*, 218–224. (d) Nilsson, M.; Cabaleiro-Lago, C.; Valente, A. J. M.; Soederman, O. *Langmuir* **2006**, *22*, 8663–8669.

(40) (a) Buffy, J. J.; Waring, A. J.; Hong, M. *J. Am. Chem. Soc.* **2005**, *127*, 4477–4483. (b) Martinek, T. A.; Hetenyi, A.; Fulop, L.; Mandity, I. M.; Toth, G. K. *Angew. Chem., Int. Ed.* **2006**, *45*, 2396–2400. (c) Luo, W.; Hong, M. *J. Am. Chem. Soc.* **2006**, *128*, 7242–7251. (d) Salgado, E. N.; Faraone-Mennella, J.; Tezcan, F. A. *J. Am. Chem. Soc.* **2007**, *129*, 13374–13375.

TABLE 2. Diffusion Coefficients (D), Derived from the Probe α-CH_2 Peaks, of the Most Abundant Assemblies Formed in $CDCl_3/CD_3OD$ (2:1, v/v; 298 K) from Mixtures of *p*-, *m*-, and *o*-1 (10 mM)/C_{10} at Different Molar Ratios

		D ($\times 10^{-5}$ cm^2 s^{-1})					
		host/guest molar ratio					
system pair	species	1:0.5	1:0.67	1:1	1:1.5	1:2	1:4
p-**1**/C_{10}	type C	0.20 ± 0.01					
	type D (p = 2)		0.14 ± 0.01	0.15 ± 0.01	0.14 ± 0.01	0.14 ± 0.01	
	type B				0.20 ± 0.01	0.21 ± 0.01	0.23 ± 0.01
	picrate	0.61 ± 0.01	0.48 ± 0.01	0.48 ± 0.01	0.47 ± 0.01	0.47 ± 0.01	0.49 ± 0.01
m-**1**/C_{10}	type C	0.20 ± 0.01					
	type D (p = 2)		0.17 ± 0.01	0.15 ± 0.01	0.15 ± 0.01	0.15 ± 0.01	
	type B				0.20 ± 0.01	0.20 ± 0.01	0.20 ± 0.01
o-**1**/C_{10}	type C	0.21 ± 0.01	0.21 ± 0.01				
	types C and D			0.18 ± 0.01	0.18 ± 0.01	0.16 ± 0.01	
	type B			0.22 ± 0.01	0.23 ± 0.01	0.22 ± 0.01	0.21 ± 0.01
				C_{10} (10 mM)			**C_{10}** (40 mM)
C_{10}·2Pic	picrate			0.59 ± 0.01			0.53 ± 0.01

presence of an excess of guest, these species broke down, ultimately forming the 1:2 bis-*endo*-cavity assembly (*p*-**1**:C_{10} = 1:2−1:4).

The stack plots and diagram of the natural logarithm of the normalized signal decays (ln I/I_0) as a function of the diffusion weighting b values (see the Experimental Section for details) for the α-CH_2 peaks (δ = −1.30 and −1.19 ppm), from which the diffusion coefficients were extracted, are shown in Figure 3.

Failure to detect the 1:1 *endo*-cavity complex, previously observed at [*p*-**1**] = [C_{10}] = 1 mM in the ^{1}H NMR dilution experiment (see above) is ascribed to the different experimental conditions (solvent and concentration) employed during the diffusion studies. It is reasonable to assume that a 10-fold

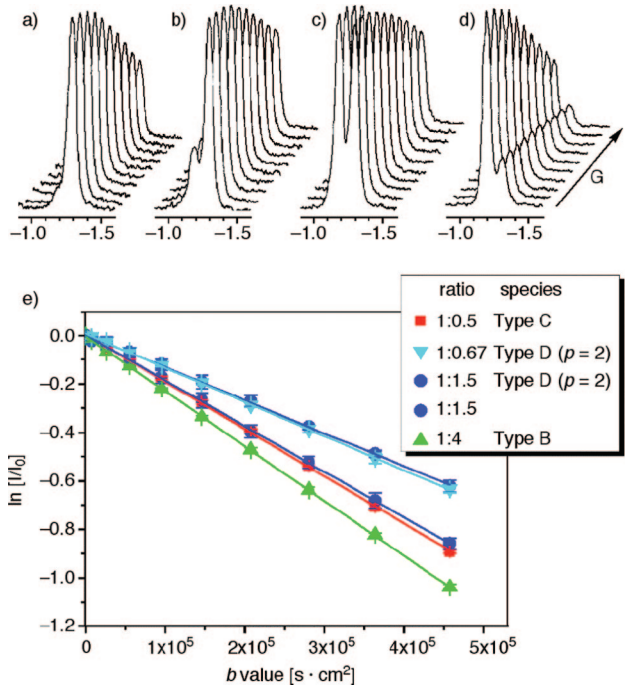

FIGURE 3. ^{1}H NMR (400 MHz; $CDCl_3/CD_3OD$, 2:1, v/v; 298 K) signal decay as a function of the gradient strength (G) relative to the α-CH_2 peaks (δ = −1.30 and −1.19 ppm) of the *p*-**1** (10 mM)/C_{10} assemblies formed at different molar ratios: (a) 1:0.5; (b) 1:0.67; (c) 1:1.5; (d) 1:4; and (e) plot of the natural logarithm of the normalized signal decay (ln I/I_0) of the peaks shown in traces a−d of *p*-**1**/C_{10} 1:0.5 (red ■), *p*-**1**/C_{10} 1:0.67 (light blue ▼), *p*-**1**/C_{10} 1:1.5 (blue ●), and *p*-**1**/C_{10} 1:4 (green ▲) as a function of the b values.

concentration increase (10 vs 1 mM) tends to favor the polycapsular association of the complementary pair over the simple 1:1 *endo*-cavity complex. The latter, on the other hand, does form under these conditions (e.g., in the case of the *p*-**1**/C_8 pair, see Table 1) but only when the dication guest is not long enough to span the cavities of two host molecules.

An additional proof in favor of the above-described assembling modes of the *p*-**1**/C_{10} pair, and in particular for the formation of the type C assembly at high host/guest ratio, is provided by the analysis of the diffusion coefficients of the picrate anion. Data in Table 2 indicate that in the presence of the type C assembly (e.g., *p*-**1**:C_{10} = 1:0.5) ion pairing of the picrate anion with the diammonium counterion is prevented by the encapsulation of the latter within two bis-calixarene units. Accordingly, the D values calculated from the peaks of these two ions (δ = 8.76 and −1.30 ppm for the picrate and α-CH_2 ≡ α′-CH_2 of C_{10}, respectively) are markedly different. On the other hand, when type D assemblies (e.g., *p*-**1**:C_{10} = 1:1) or the type B complex (e.g., *p*-**1**:C_{10} = 1:4) are formed, since either one or two *exo*-cavity ammonium moiet(y)ies (is)are available, ion pairing of the picrate ions present in solution can now take place. Consequently, the diffusion coefficient of the latter sensibly decreases (D = (0.48−0.49 ± 0.01) × 10^{-5} cm^2 s^{-1}) relative to the free salt as such (D = (0.53−0.59 ± 0.01) × 10^{-5} cm^2 s^{-1}).

With the aim of understanding the role played by the different *p*-, *m*-, and *o*-xylyl linkages on the host structure and ultimately revealing a scale of self-assembly reactivity of the latter, diffusion studies were then extended to bis-calix[5]arenes *m*-**1** and *o*-**1**. In keeping with the ^{1}H NMR titration/dilution findings, diffusion data for these two hosts, upon addition of C_{10}·2Pic (see Tables S5 and S6, see the Supporting Information), clearly show that both pairs (*m*-**1**/C_{10} and *o*-**1**/C_{10}) spontaneously self-assemble into different species in the same way that *p*-**1**/C_{10} does. The diagram shown in Figure 4 reports the diffusion coefficients—calculated from the decay of the α-CH_2 signals—for the most abundant species formed in solutions by the **1**/C_{10} pairs at different molar ratios (Table 2 and Tables S5 and S6 in the Supporting Information). This plot shows that, overall, the three pairs have, at a given ratio, very similar diffusion coefficients.

One small difference that emerges, however, concerns the slightly higher diffusion coefficients observed for the assemblies formed, at a 1:1 ratio, from *o*-**1** and C_{10} (D = (0.18−0.22 ± 0.01) × 10^{-5} cm^2 s^{-1}) in comparison with the other two isomeric hosts *p*- and *m*-**1** (D = (0.15 ± 0.01) × 10^{-5} cm^2 s^{-1}). The D

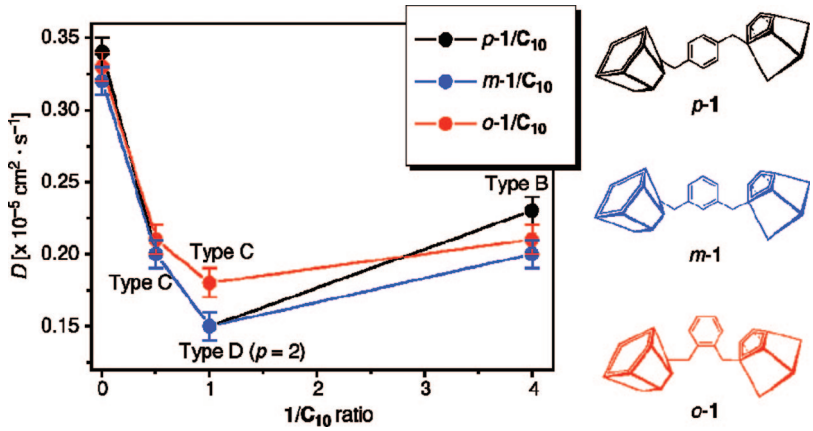

FIGURE 4. Plot of the diffusion coefficients, relative to the α-CH_2 peaks ($\delta = -1.30$ and -1.19 ppm), of the assemblies formed in $CDCl_3/CD_3OD$ (2:1, v/v; 298 K) as a function of the **1** (10 mM)/$\mathbf{C_{10}}$ molar ratio: *p*-**1**/$\mathbf{C_{10}}$ (black ●), *m*-**1**/$\mathbf{C_{10}}$ (blue ●), *o*-**1**/$\mathbf{C_{10}}$ (red ●).

values detected in the case of *o*-**1**/$\mathbf{C_{10}}$ suggest that under these conditions, the polycapsular assemblies formed (if any) are smaller. These results are likely due to the structural differences of the bis-calix[5]arenes under study, and in particular to the steric hindrance of the two cavities and/or the unfavorable bridging angle present in the *o*-**1** isomer that make the growth of a linear polycapsular assembly not efficient.

Determination of the Association Constants. In order to gain a deeper understanding of the multiple self-assembly processes taking place in solution between the **1**/$\mathbf{C}_n$ complementary pairs, the association constants of the discrete supramolecular species formed were estimated (by ^{1}H NMR spectroscopy), with the final aim of assessing a relative scale of stabilities. For supramolecular assemblies derived from homoditopic host/guest components, binding constant determination is not straightforward as several species (e.g., polycapsules) may come simultaneously into play in setting up a complex multiequilibrium system. Furthermore, in the specific case of neutral hosts and saline guests, the concomitant association equilibrium between the charged guest and its counterion (i.e., ion-pairing) has also to be taken into account, particularly when low polarity media are employed.[23a,46] However, by taking advantage of the dynamic behavior of the systems under study and the slow exchange regime—on the NMR time scale—between free and complexed species, we were able to set up a series of tailor-made ^{1}H NMR titration experiments which enabled us to estimate the conditional association constants of type A, B, and C assemblies. In practice, host and guest were mixed together so as to yield, upon equilibration under fixed conditions (vide infra), a given set of species. Their equilibrium concentrations in solution were then directly measured (via integration of selected peaks) and their values subsequently inputted into the pertinent equations reported below (eqs 3−5).

Two different sets of equilibria were considered:

$$2\mathbf{1} + \mathbf{C}_n \overset{K_{1(A)}}{\rightleftharpoons} \mathbf{1} + \mathbf{C}_n \subset \mathbf{1} \overset{K_{2(C)}}{\rightleftharpoons} \mathbf{1} \supset \mathbf{C}_n \subset \mathbf{1} \qquad (1)$$

$$\mathbf{1} + 2\mathbf{C}_n \overset{K_{1(A)}}{\rightleftharpoons} \mathbf{C}_n + \mathbf{C}_n \subset \mathbf{1} \overset{K_{2(B)}}{\rightleftharpoons} \mathbf{C}_n \subset \mathbf{1} \supset \mathbf{C}_n \qquad (2)$$

Equilibria eqs 1 and 2 account for the two consecutive association events leading to the initial formation of type A assembly and then to either of the two trimolecular type C or type B species, derived from the uptake of a second host molecule in one case and guest molecule in the other. $K_{1(A)}$ is the conditional association constant for the formation of type A assembly, whereas $K_{2(C)}$ and $K_{2(B)}$ refer to those related to the conversion of type A into type C and B assemblies, respectively.

^{1}H NMR measurements were carried out in $CDCl_3/CD_3OD$ (2:1, v/v) solutions at a fixed 1 mM $\mathbf{C}_n\cdot$2Pic concentration, to make sure salt association/dissociation played a constant role throughout the experiments. Accordingly, to favor the formation of only certain species at a time, *p*-, *m*- and *o*-**1** concentration was set to 0.25 mM, 1 mM, and 2 mM for $K_{2(B)}$, $K_{1(A)}$, and $K_{2(C)}$ determination, respectively. Furthermore, to simplify the picture by avoiding (poly)capsular formation, under the assumption that the two $\mathbf{C_8}\cdot$2Pic and $\mathbf{C_{10}}\cdot$2Pic salts display comparable dissociation constants and their dication exhibit similar affinities for receptors **1**, the shorter guest $\mathbf{C_8}$ was used instead of $\mathbf{C_{10}}$ for the determination of $K_{1(A)}$ and $K_{2(B)}$.

The conditional association constants would then take the following forms:

$$K_{1(A)} = [\mathbf{C_8} \subset \mathbf{1}]/[\mathbf{1}][\mathbf{C_8}] \qquad (3)$$

$$K_{2(C)} = [\mathbf{1} \supset \mathbf{C_{10}} \subset \mathbf{1}]/[\mathbf{1}][\mathbf{C_{10}} \subset \mathbf{1}] \qquad (4)$$

$$K_{2(B)} = [\mathbf{C_8} \subset \mathbf{1} \supset \mathbf{C_8}]/[\mathbf{C_8} \subset \mathbf{1}][\mathbf{C_8}] \qquad (5)$$

Data in Table 3 indicate that *m*-**1** and *p*-**1** bind $\mathbf{C_8}/\mathbf{C_{10}}$ more efficiently than *o*-**1**. In the three cases, formation of the 1:1 *endo*-cavity type A complex is only slightly favored over its subsequent conversion to the monocapsular type C complex ($K_{1(A)} > K_{2(C)}$). Conversion of type A into type B complexes,

(41) (a) Greenwald, M.; Wessely, D.; Goldberg, I.; Cohen, Y. *New J. Chem.* **1999**, *23*, 337–344. (b) Shaul, M.; Cohen, Y. *J. Org. Chem.* **1999**, *64*, 9358–9364. (c) Allouche, L.; Marquis, A.; Lehn, J.-M. *Chem.—Eur. J.* **2006**, *12*, 7520–7525.

(42) (a) Avram, L.; Cohen, Y. *J. Am. Chem. Soc.* **2002**, *124*, 15148–15149. (b) Avram, L.; Cohen, Y. *Org. Lett.* **2003**, *5*, 1099–1102. (c) Avram, L.; Cohen, Y. *Org. Lett.* **2003**, *5*, 3329–3332. (d) Avram, L.; Cohen, Y. *J. Am. Chem. Soc.* **2004**, *126*, 11556–11563. (e) Morozova, J. E.; Kazakova, E. K.; Gubanov, E. P.; Makarova, N. A.; Archipov, V. P.; Timoshina, T. V.; Idijatullin, Z. S.; Habicher, W. D.; Konovalov, A. I. *J. Inclusion Phenom.* **2006**, *55*, 173–183. (f) Evan-Salem, T.; Baruch, I.; Avram, L.; Cohen, Y.; Palmer, L. C.; Rebek, J., Jr. *Proc. Natl. Acad. Sci. U.S.A.* **2006**, *103*, 12296–12300. (g) Evan-Salem, T.; Cohen, Y. *Chem.—Eur. J.* **2007**, *13*, 7659–7663.

(43) (a) Kaucher, M. S.; Lam, Y.-F.; Pieraccini, S.; Gottarelli, G.; Davis, J. T. *Chem.—Eur. J.* **2005**, *11*, 164–173. (b) Evan-Salem, T.; Frish, L; van Leeuwen, F. W. B.; Reinhoudt, D. N.; Verboom, W.; Kaucher, M. S.; Davis, J. T.; Cohen, Y. *Chem.—Eur. J.* **2007**, *13*, 1969–1977.

(44) (a) Moon, K.; Kaifer, A. E. *Org. Lett.* **2004**, *6*, 185–188. (b) Ko, Y. H.; Kim, K.; Kang, J.-K.; Chun, H.; Lee, J. W.; Sakamoto, S.; Yamaguchi, K.; Fettinger, J. C.; Kim, K. *J. Am. Chem. Soc.* **2004**, *126*, 1932–1933.

TABLE 3. Conditional Association Constants ($K_{1(A)}$, $K_{2(B)}$, and $K_{2(C)}$; See Main Text for Details) and Percentage of Complexation, Determined by ^{1}H NMR (300 MHz; $CDCl_3/CD_3OD$ 2:1, v/v; 295 K), for Hosts *p*-, *m*-, and *o*-1 and α,ω-Alkanediyldiammonium Dipicrate Guest Salts (C_n·2Pic) (Values Are Reported in M^{-1})

	p-**1**	*m*-**1**	*o*-**1**
$K_{1(A)}$[a]	$(3.8 \pm 1.0) \times 10^4$	$(3.7 \pm 0.9) \times 10^4$	$(1.8 \pm 0.3) \times 10^4$
% complexation[b]	85.0	84.9	79.2
$K_{2(C)}$[c]	$(2.0 \pm 0.5) \times 10^4$	$(2.1 \pm 0.2) \times 10^4$	$(7.0 \pm 0.6) \times 10^3$
% complexation[b]	80.0	80.4	68.6
$K_{2(B)}$[a]	$(3.9 \pm 0.1) \times 10^2$	$(1.5 \pm 0.4) \times 10^2$	$(1.1 \pm 0.2) \times 10^2$
% complexation[b]	21.3	9.6	7.7

[a] Determined in the presence of $\mathbf{C_8}$·2Pic. [b] Average of three experiments. [c] Determined in the presence of $\mathbf{C_{10}}$·2Pic.

on the other hand, is definitely more difficult and accordingly takes place with binding constants of about 2 orders of magnitude lower ($K_{2(B)} \ll K_{1(A)}$). Overall, these results are consistent with a bimolecular or trimolecular "mono-cavity" self-assembly process (i.e., type A or C, respectively) being much more favored over the "bis-cavity" one (i.e., type B), presumably as a result of a less demanding guest-induced conformational change of the receptor and/or a lower electrostatic repulsion between facing positive charges hosted by a single receptor molecule. In relative terms and in agreement with the diffusion NMR findings, the lower affinity displayed by *o*-**1** for alkanediyldiammonium ions can likely be ascribed to the additional structural constraints deriving from a more pronounced steric hindrance between the two nearby cavities and/or their tighter bridging angle.

Conclusions

Taken together, the evidence collected in the present study indicates that modular pairs of complementary bis-calix[5]arenes **1** and α,ω-alkanediyldiammonium ions, of an appropriate length (H_3N^+-$(CH_2)_n$-NH_3^+, $n \geq 10$), self-assemble spontaneously and afford a variety of supramolecular species ((bis-)*endo*-cavity and (poly)capsular assemblies) as a result of single to multiple intermolecular inclusion events. Assembly/disassembly of these homoditopic complementary molecules takes place in a dynamic fashion and, because of this, product composition can be reversibly directed toward the desired species by basic external inputs (e.g., variation of the concentration and/or molar ratio of the two components). In solution, the three isomeric hosts **1** (10−50 mM) in the presence of a defect (≤0.5 equiv) of 1,10-decanediyldiammonium dipicrate $\mathbf{C_{10}}$·2Pic form almost exclusively monocapsular assemblies (type C). By increasing the amount of salt, so as to reach a 1:1 host/guest ratio, these species produce oligo- to polycapsular assemblies (type D, $p > 1$). In 2:1 $CDCl_3/CD_3OD$ solutions, further salt addition (up to a 1:4 host (10 mM)/guest molar ratio) induces supramolecular reorganization and ultimately yields bis-*endo*-cavity assemblies (type B). In 9:1 $CDCl_3/CD_3OD$, on the other hand, fifty-fold dilution of [**1**] = [$\mathbf{C_{10}}$] = 50 mM solutions generates first 1:1 *endo*-cavity complexes (type A) and then, in turn, type B or C species as either the salt or the host stoichiometry is increased to the appropriate value (i.e., **1**:$\mathbf{C_{10}}$ = 1:4 or 4:1, respectively). ^{1}H NMR data on the conditional association constants of these last two species suggest that their formation (via their intermediate type A species) proceeds with a negative cooperativity effect.

This complex self-assembly behavior of the **1**/$\mathbf{C_{10}}$ complementary pairs has been elucidated by a combination of ESI-MS, ^{1}H NMR, and diffusion NMR studies each providing key elements to the understanding of the overall scenario. ESI-MS analysis, for instance, has confirmed that dynamic self-assembly of bis-calixarenes and diammonium ions also takes place in the gas phase where, in addition to the four distinct species observed in solution, collections of mixed bis-*endo*-cavity assemblies were detected upon exposure of **1** to equimolar mixtures of the five diammonium salts ($\mathbf{C_8}$−$\mathbf{C_{12}}$·2Pic). ^{1}H NMR observations based on complexation induced shifts and integration of symmetry-related probe resonances have been of paramount value for structural elucidation and association constant determination. Similarly, diffusion NMR has been a crucial tool for the identification of the different assemblies formed at different stoichiometries and particularly in pinning-down the smaller size of the assemblies derived from *o*-**1** as compared to those formed by *p*-**1** and *m*-**1**.

Overall, our account outlines a general strategy (applicable in principle to other complementary homoditopic host−guest pairs) for constructing noncovalent assemblies of the desired composition and then controlling their interconversion into one another. Now that the basic self-assembly dynamics of these systems have been revealed and understood, fine-tuning of the structural features of these prototypical pairs should allow us to prepare species (e.g., supramolecular polymers and capsules) with potential applications in the field of materials science, drug delivery, and analyte sensing/transport.

Experimental Section

General Synthetic Procedure for Compounds *o*-, *m*-, and *p*-3. A suspension of **2** (0.81 g, 1.0 mmol) and CsF (0.76 g, 5.0 mmol) in DMF (50 mL) was stirred at 50 °C for 1 h and then cooled at rt. The appropriate α,α′-dibromoxylene (0.12 g, 0.5 mmol) in DMF (40 mL) was added dropwise, and the resulting mixture was stirred at rt for an additional period of 24−48 h. Solvent removal under reduced pressure gave a residue which was partitioned between water and CH_2Cl_2. The organic layer was separated, dried over $MgSO_4$, and concentrated. The resulting oil was purified by CC to afford, after crystallization from the appropriate solvent, bis-calixarene octols **3**.

Bis-calixarene Octol *o*-3. Obtained in 56% yield after CC (toluene) and crystallization: mp 198−201 °C (from toluene); ^{1}H NMR δ 1.05, 1.24, 1.29 (s, 1:2:2, 90 H, $C(CH_3)_3$), 3.38 and 4.02 (AX system, J = 14.0 Hz, 8 H, $ArCH_2Ar$), 3.45 and 4.41 (AX system, J = 14.0 Hz, 8 H, $ArCH_2Ar$), 3.49 and 4.08 (AX system, J = 14.1 Hz, 4 H, $ArCH_2Ar$), 5.55 (s, 4 H, Xy-CH_2), 7.13 (s, 4 H, *Ar*), 7.17−7.19 (m, 16 H, *Ar*), 7.58−7.61 and 7.94−7.98 (AA′BB′ system, 4 H, *Xy*), 7.65 and 7.81 (br s, 1:1, 8 H, OH) ppm; ^{13}C NMR δ 30.8, 31.1, 31.2, 31.4, 31.5, 33.81, 33.82, 34.1, 75.3, 125.3, 125.4, 125.7, 125.8, 126.0, 126.20, 126.24, 126.4, 126.8, 129.3, 129.9, 132.0, 135.1, 142.5, 143.7, 147.4, 147.5, 149.2, 150.6 ppm; ESI-MS m/z 1725 $[M + H]^+$. Anal. Calcd for $C_{118}H_{146}O_{10}$: C, 82.19; H, 8.53. Found: C, 81.87; H, 8.80.

(45) (a) Timmerman, P.; Weidmann, J.-L.; Jolliffe, K. A.; Prins, L. J.; Reinhoudt, D. N.; Shinkai, S.; Frish, L.; Cohen, Y. *J. Chem. Soc., Perkin Trans. 2* **2000**, 2077–2089. (b) Bukhaltsev, E.; Frish, L.; Cohen, Y.; Vigalok, A. *Org. Lett.* **2005**, *7*, 5123–5126. (c) Gulino, F. G.; Lauceri, R.; Frish, L.; Evan-Salem, T.; Cohen, Y.; De Zorzi, R.; Geremia, S.; Di Costanzo, L.; Randaccio, L.; Sciotto, D.; Purrello, R. *Chem.−Eur. J.* **2006**, *12*, 2722–2729.

(46) For the role played by counterions in cation species complexation see: (a) Roelens, S.; Torriti, R. *J. Am. Chem. Soc.* **1998**, *120*, 12443–12452. (b) Bartoli, S.; Roelens, S. *J. Am. Chem. Soc.* **1999**, *121*, 11908–11909. (c) Böhmer, V.; Dalla Cort, A.; Mandolini, L. *J. Org. Chem.* **2001**, *66*, 1900–1902. (d) Bartoli, S.; Roelens, S. *J. Am. Chem. Soc.* **2002**, *124*, 8307–8315. (e) Arduini, A.; Brindani, E.; Giorgi, G.; Pochini, A.; Secchi, A. *J. Org. Chem.* **2002**, *67*, 6188–6194. (f) Jones, J. W.; Gibson, H. W. *J. Am. Chem. Soc.* **2003**, *125*, 7001–7004. (g) Huang, F.; Jones, J. W.; Slebodnick, C.; Gibson, H. W. *J. Am. Chem. Soc.* **2003**, *125*, 14458–14464. (i) Sarri, P.; Venturi, F.; Cuda, F.; Roelens, S. *J. Org. Chem.* **2004**, *69*, 3654–3661. (j) Clemente-León, M.; Pasquini, C.; Hebbe-Viton, V.; Lacour, J.; Dalla Cort, A.; Credi, A. *Eur. J. Org. Chem.* **2006**, 105–112. (k) Huang, F.; Jones, J. W.; Gibson, H. W. *J. Org. Chem.* **2007**, *72*, 6573–6576.

Bis-calixarene Octol *m*-3. Obtained in 58% yield after CC (*n*-hexane/$CHCl_3$, 2:1 to 1:2 v/v): mp 191−194 °C (from CH_3CN/CH_2Cl_2); ^{1}H NMR δ 1.07, 1.23, 1.27 (s, 1:2:2, 90 H, C(CH_3)$_3$), 3.37 and 4.06 (AX system, J = 14.0 Hz, 8 H, ArCH_2Ar), 3.43 and 4.02 (AX system, J = 14.3 Hz, 4 H, ArCH_2Ar), 3.50 and 4.49 (AX system, J = 13.8 Hz, 8 H, ArCH_2Ar), 5.30 (s, 4 H, Xy-CH_2), 7.13 (s, 4 H, *Ar*), 7.15−7.19 (m, 16 H, *Ar*), 7.70 (t, J = 7.6 Hz, 1 H, *Xy*), 7.74, 7.84 (br s, 1:1, 8 H, OH), 7.89 (dd, J = 7.6, 1.6 Hz, 2 H, *Xy*), 8.00 (br s, 1 H, *Xy*) ppm; ^{13}C NMR δ 30.7, 31.1, 31.2, 31.4, 31.5, 33.8, 34.1, 77.2, 125.38, 125.42, 125.7, 125.8, 126.0, 126.3, 126.4, 126.8, 127.6, 128.3, 129.5, 132.2, 136.9, 142.6, 143.7, 147.52, 147.55, 149.1, 150.1 ppm; ESI-MS m/z 1725 $[M + H]^+$. Anal. Calcd for $C_{118}H_{146}O_{10}$: C, 82.19; H, 8.53. Found: C, 81.78; H, 8.79.

Bis-calixarene Octol *p*-3. Obtained in 44% yield after CC (toluene) and crystallization: mp 207−210 °C (from CH_3CN/CH_2Cl_2); ^{1}H NMR δ 1.08, 1.22, 1.27 (s, 1:2:2, 90 H), 3.37 and 4.08 (AX system, J = 14.0 Hz, 8 H, ArCH_2Ar), 3.41 and 4.03 (AX system, J = 14.0 Hz, 4 H, ArCH_2Ar), 3.48 and 4.47 (AX system, J = 13.8 Hz, 8 H, ArCH_2Ar), 5.25 (s, 4 H, Xy-CH_2), 7.13−7.20 (m, 20 H, *Ar*), 7.69, 7.81 (br s, 1:1, 8 H, OH), 7.85 (s, 4 H) ppm; ^{13}C NMR δ 30.8, 31.2, 31.36, 31.43, 31.6, 33.84, 33.86, 34.1, 77.2, 125.4, 125.7, 125.8, 126.0, 126.3, 126.42, 126.46, 126.9, 128.6, 132.2, 136.7, 142.6, 143.7, 147.5, 147.6, 149.2, 150.1 ppm; ESI-MS m/z 1725 $[M + H]^+$. Anal. Calcd for $C_{118}H_{146}O_{10}$: C, 82.19; H, 8.53. Found: C, 81.95; H, 8.69.

General Synthetic Procedure for Compounds *o*-, *m*-, and *p*-1. A mixture of octol **3** (0.60 g, 0.35 mmol), 4-methylpentyl tosylate (2.69 g, 10.50 mmol), and anhydrous K_2CO_3 (1.45 g, 10.50 mmol) in CH_3CN (70 mL) was stirred under reflux for 8 days. Excess base and inorganic salts were collected by filtration and thoroughly washed with CH_2Cl_2. The combined organic layer was concentrated, and the residual solid was triturated with MeOH, collected by suction filtration, and recrystallized to afford bis-calixarene **1**.

Bis-calixarene *o*-1: 62% yield; mp 216−219 °C (from CH_3CN/$CHCl_3$); ^{1}H NMR δ 0.75, 0.941, 1.24 (s, 1:2:2, 90 H, C(CH_3)$_3$), 0.91, 0.943 (d, J = 6.7 Hz, 1:1, 48 H, CH(CH_3)$_2$), 1.18−1.38 (m, 16 H), 1.47−1.65 (m, 8 H), 1.71−1.94 (m, 16 H), 3.05 and 4.37 (AX system, J = 14.0 Hz, 8 H, ArCH_2Ar), 3.22 and 4.54 (AX system, J = 13.8 Hz, 8 H, ArCH_2Ar), 3.26 and 4.52 (AX system, J = 13.8 Hz, 4 H, ArCH_2Ar), 3.35−3.50 (m, 8 H, OCH_2), 3.62−3.76 (m, 8 H, OCH_2), 4.63 (s, 4 H, Xy-CH_2), 6.61 (s, 4 H, *Ar*), 6.81 and 6.82 (ABq, J = 2.4 Hz, 8 H, *Ar*), 7.09 and 7.13 (ABq, J = 2.3 Hz, 8 H, *Ar*), 7.36−7.39 and 7.81−7.84 (AA′BB′ system, 4 H, *Xy*) ppm; ^{13}C NMR δ 22.7, 22.8, 22.9, 23.0, 28.18, 28.26, 28.31, 28.35, 29.2, 29.6, 29.8, 31.1, 31.3, 31.6, 33.8, 33.9, 34.0, 35.0, 35.1, 72.7, 73.7, 74.4, 124.4, 124.8, 125.2, 126.0, 126.2, 127.8, 129.4, 133.3, 133.5, 133.9, 134.0, 134.2, 135.8, 144.41, 144.43, 144.9, 151.9, 152.6, 153.1 ppm; ESI-MS m/z 2414.0 $[(M + NH_4)]^+$, 1215.9 $[(M + 2NH_4)]^{2+}$. Anal. Calcd for $C_{166}H_{242}O_{10}$: C, 83.15; H, 10.17. Found: C, 83.45; H, 10.36.

Bis-calixarene *m*-1: 73% yield; mp 240−243 °C (from MeOH/CH_2Cl_2); ^{1}H NMR δ 0.81, 0.97, 1.21 (s, 1:2:2, 90 H, C(CH_3)$_3$), 0.88, 0.89, 0.93 (d, J = 6.5 Hz, 1:1:2, 48 H, CH(CH_3)$_2$), 1.09−1.43 (m, 16 H), 1.47−1.65 (m, 8 H), 1.72−1.93 (m, 16 H), 3.18 and 4.50 (AX system, J = 14.2 Hz, 8 H, ArCH_2Ar), 3.23 and 4.55 (AX system, J = 13.8 Hz, 8 H, ArCH_2Ar), 3.27 and 4.53 (AX system, J = 13.5 Hz, 4 H, ArCH_2Ar), 3.42−3.71 (m, 16 H, OCH_2), 4.79 (s, 4 H, Xy-CH_2), 6.68 (s, 4 H, *Ar*), 6.83 and 6.85 (ABq, J = 2.5 Hz, 8 H, *Ar*), 7.08 and 7.10 (ABq, J = 2.5 Hz, 8 H, *Ar*), 7.18 (s, 1 H, *Xy*), 7.39 (t, J = 7.9 Hz, 1 H, *Xy*) 7.63 (d, J = 7.9 Hz, 2 H, *Xy*) ppm; ^{13}C NMR δ 22.74, 22.78, 22.83, 22.9, 28.17, 28.18, 28.24, 28.3, 29.4, 29.6, 31.2, 31.3, 31.5, 33.8, 33.9, 34.0, 35.0, 35.1, 74.0, 74.3, 75.5, 124.7, 124.9, 125.2, 125.9, 126.0, 127.6, 127.7, 127.9, 133.5, 133.6, 133.7, 134.07, 134.12, 138.0, 144.4, 144.5, 144.8, 151.7, 152.6, 153.1 ppm; ESI-MS m/z 2414.0 $[(M + NH_4)]^+$, 1215.9 $[(M + 2NH_4)]^{2+}$. Anal. Calcd for $C_{166}H_{242}O_{10}$: C, 83.15; H, 10.17. Found: C, 83.47; H, 10.39.

Bis-calixarene *p*-1: 58% yield; mp 272−274 °C (from CH_3CN/CH_2Cl_2); ^{1}H NMR δ 0.83, 0.97, 1.19 (s, 1:2:2, 90 H), 0.87, 0.88, 0.93 (d, J = 6.6 Hz, 1:1:2, 48 H), 1.2−1.4 (m, 8 H), 1.48−1.66 (m, 16 H), 1.71−1.93 (m, 16 H), 3.18 and 4.51 (AX system, J = 13.8 Hz, 8 H, ArCH_2Ar), 3.23 and 4.54 (AX system, J = 13.8 Hz, 8 H, ArCH_2Ar), 3.26 and 4.53 (AX system, J = 13.5 Hz, 4 H, ArCH_2Ar), 3.44−3.54 (m, 8 H, OCH_2), 3.61−3.67 (m, 8 H, OCH_2), 4.82 (s, 4 H, Xy-CH_2), 6.70 (s, 4 H, *Ar*), 6.85, 7.08, (pseudo-s, 1:1, 16 H, *Ar*), 7.45 (s, 4 H, *Xy*) ppm; ^{13}C NMR δ 22.75, 22.79, 22.84, 22.9, 28.18, 28.21, 28.23, 28.3, 29.3, 29.7, 31.2, 31.3, 31.5, 33.8, 33.9, 34.0, 35.0, 35.1, 74.0, 74.3, 75.6, 124.8, 125.0, 125.2. 125.9, 126.0, 128.2, 133.60, 133.64, 133.8, 134.05, 134.08, 137.5, 144.45, 144.47, 144.8, 151.8, 152.6, 153.1 ppm; ESI-MS m/z 2414.0 $[(M + NH_4)]^+$, 1215.9 $[(M + 2NH_4)]^{2+}$. Anal. Calcd for $C_{166}H_{242}O_{10}$: C, 83.15; H, 10.17. Found: C, 83.52; H, 10.49.

Acknowledgment. We are grateful to MiUR (PRIN-2006 project) for financial support of this work.

Supporting Information Available: General experimental methods and diffusion NMR, ESI-MS, NMR titration/dilution procedures. ESI-MS spectra of *o*-**1**/$\mathbf{C_{10}}$ pair and *o*-**1**/$\mathbf{C_8}$–$\mathbf{C_{12}}$ mixture. ESI-MS peak assignments of the 15 couples of modular components **1**/$\mathbf{C_8}$–$\mathbf{C_{12}}$, ^{1}H NMR peak assignment for the selected probe groups of the **1**/$\mathbf{C_{10}}$ pairs, and ^{1}H NMR spectra of the *p*-, *m*-, and *o*-**1**/$\mathbf{C_{10}}$ assemblies. Diffusion coefficients of the assemblies formed at different *p*-, *m*-, and *o*-**1**/$\mathbf{C_{10}}$ ratios, as well as diffusion coefficients of *p*-**1** and $\mathbf{C_{10}}$ at different concentrations. ^{1}H and ^{13}C NMR spectra of compounds *o*-, *m*-, and *p*-**3** and *o*-, *m*-, and *p*-**1**. This material is available free of charge via the Internet at http://pubs.acs.org.

JO801202H